JOURNAL OF VIROLOGY, Mar. 2010, p. 2935–2945 Vol. 84, No. 6
0022-538X/10/$12.00 doi:10.1128/JVI.00757-09

GLTSCR2/PICT-1, a Putative Tumor Suppressor Gene Product, Induces the Nucleolar Targeting of the Kaposi's Sarcoma-Associated Herpesvirus KS-Bcl-2 Protein▽

Inna Kalt, Tatyana Borodianskiy-Shteinberg, Adi Schachor, and Ronit Sarid*

The Mina and Everard Goodman Faculty of Life Sciences, Bar Ilan University, Ramat-Gan, Israel

Received 14 April 2009/Accepted 7 December 2009

KS-Bcl-2, encoded by Kaposi's sarcoma-associated herpesvirus (KSHV), is a structural and functional homologue of the Bcl-2 family of apoptosis regulators. Like several other Bcl-2 family members, KS-Bcl-2 protects cells from apoptosis and autophagy. Using a yeast two-hybrid screen and coimmunoprecipitation assays, we identified a novel KS-Bcl-2-interacting protein, referred to as protein interacting with carboxyl terminus 1 (PICT-1), encoded by a candidate tumor suppressor gene, GLTSCR2. Confocal laser scanning microscopy revealed nucleolar localization of PICT-1, whereas KS-Bcl-2 was located mostly at the mitochondrial membranes with a small fraction in the nucleoli. Ectopic expression of PICT-1 resulted in a large increase in the nucleolar fraction of KS-Bcl-2, and only a minor fraction remained in the cytoplasm. Furthermore, knockdown of endogenous PICT-1 abolished the nucleolar localization of KS-Bcl-2. However, ectopically expressed PICT-1 did not alter the cellular distribution of human Bcl-2. Subsequent analysis mapped the crucial amino acid sequences of both KS-Bcl-2 and PICT-1 required for their interaction and for KS-Bcl-2 targeting to the nucleolus. Functional studies suggest a correlation between nucleolar targeting of KS-Bcl-2 by PICT-1 and reduction of the antiapoptotic activity of KS-Bcl-2. Thus, these studies demonstrate a cellular mechanism to sequester KS-Bcl-2 from the mitochondria and to downregulate its virally encoded antiapoptotic activity. Additional characterization of the interaction of KS-Bcl-2 and PICT-1 is likely to shed light on the functions of both proteins.

Kaposi's sarcoma (KS)-associated herpesvirus (KSHV), also referred to as human herpesvirus 8 (HHV-8), is a gamma 2 herpesvirus implicated in several cancers, including KS, primary effusion lymphoma (PEL), and a subset of multicentric Castleman's disease. Among human viruses, KSHV is most closely related to the Epstein-Barr virus (EBV), a tumorigenic gamma 1 herpesvirus known to be associated with lymphomas and nasopharyngeal carcinoma (10, 12).

KSHV open reading frame 16 (orf16) encodes the KS-Bcl-2 protein, which shares sequence and functional homology with the Bcl-2 family (9, 31). Members of the Bcl-2 family are defined by the presence of up to four conserved domains known as the Bcl-2 homology (BH) domains. Several members also possess a carboxy-terminal transmembrane domain that mediates their association with intracellular membranes, such as the endoplasmic reticulum or mitochondria. Bcl-2 proteins are thought to serve primarily as cell death agonists or antagonists that integrate diverse survival and death signals, which are generated outside and within the cell (15, 37), yet Bcl-2 proteins also modulate cell cycle checkpoints, DNA repair/recombination pathways, calcium homeostasis, and cellular bioenergetics.

All gammaherpesviruses encode Bcl-2 proteins that generally share 20 to 30% homology with one another and with their cellular counterparts (8, 11). The conservation of Bcl-2 homologues in these viruses indicates their importance for viral infection, with an evolutionarily conserved function of unknown nature. KS-Bcl-2, like most herpesvirus homologues of Bcl-2, contains a transmembrane domain and demonstrates conservation of sequences in both BH1 and BH2 but has only a low degree of homology with other regions of cellular Bcl-2 (18, 22). Still, KS-Bcl-2 shares 3-dimensional structural conservation with Bcl-2 family members and includes the conserved BH3 binding groove and a hydrophobic membrane anchor domain that also contains a mitochondrial outer membrane targeting signal (18). The BH3 binding cleft of KS-Bcl-2 binds with high affinity to peptides encoding BH3 domains present on the proapoptotic proteins Noxa, Bik, PUMA, Bak, Bax, Bid, Bim, and, to a much lesser extent, Bad (13, 18, 22). Based on these characteristics, KS-Bcl-2 has been suggested to have the closest resemblance to the cellular Bcl-2 family member Mcl-1 (13).

Previous studies have demonstrated that KS-Bcl-2 protects various cell types from apoptosis mediated by the expression of BAX, tBid, or Bim through Sindbis virus infection or by ectopic expression of KSHV-cyclin-CDK6 (9, 13, 25, 31). However, unlike the cellular Bcl-2, KS-Bcl-2 is not a substrate for KSHV-cyclin-CDK6 phosphorylation (25) and cannot be converted into a proapoptotic protein via caspase cleavage (3). KS-Bcl-2 is able to form a stable complex with the cellular protein Aven, which binds Apaf-1 and is known as a regulator of caspase 9 and ataxia-telangiectasia (ATM) activation (7, 16). Like the cellular and other virus-encoded Bcl-2 proteins, KS-Bcl-2 binds Beclin and disrupts its lysosomal degradation pathway of autophagy (21, 29). However, since KS-Bcl-2 lacks the nonstructured loop located between the BH4 and BH3 domains, its binding to BH3-containing proapoptotic proteins

* Corresponding author. Mailing address: The Mina and Everard Goodman Faculty of Life Sciences, Bar Ilan University, Ramat-Gan, Israel 52900. Phone: 972-3-5317853. Fax: 972-3-7384058. E-mail: saridr@mail.biu.ac.il.

▽ Published ahead of print on 30 December 2009.

and to the BH3-containing proautophagy protein Beclin is not modulated by phosphorylation (38).

KS-Bcl-2 is transcribed during lytic virus infection (30, 31). Thus, inhibition of apoptosis and autophagy by KS-Bcl-2 may provide an attractive mechanism for prolonging the life span of KSHV-infected cells, which in turn enables increased virus production or establishment of latency. Whether the function of KS-Bcl-2 is necessary for KSHV-mediated oncogenesis is still unknown. Nevertheless, the KS-Bcl-2 protein is expressed in late-stage KS lesions but has not been detected in latent or in lytic KSHV-infected PEL cells (39).

To explore the role of KS-Bcl-2 in cell signaling, we searched for its potential cellular-protein partners. In the present study, we describe a novel interaction between KS-Bcl-2 and the protein interacting with carboxyl terminus 1 (PICT-1) cellular protein, encoded by a candidate tumor suppressor gene, GLTSCR2. We show that this interaction specifically targets KS-Bcl-2 to the nucleolus and decreases its antiapoptotic activity.

(Portions of this work were submitted to Bar Ilan Univeristy, Ramat Gan, Israel, by I. Kalt and T. Borodianskiy-Shteinberg in partial fulfillment of the requirements for the degree of Doctor of Philosophy.)

MATERIALS AND METHODS

Chemicals and antibodies. Mouse anti-hemagglutinin (HA) (HA.11) (Covance Research Products), anti-green fluorescent protein (GFP) (Covance Research Products), anti-Flag (Sigma), anti-myc (myc-Tag 9B11) (Cell Signaling Technology), and goat polyclonal anti-PICT-1 (C-20) (Santa Cruz) were used with either horseradish peroxidase-conjugated, rhodamine-conjugated anti-mouse (Jackson ImmunoResearch Laboratories, Inc.) or anti-goat (Bio-Rad Laboratories) IgG. Hygromycin was obtained from MegaPharm (San Diego, CA).

Plasmids. Full-length KS-Bcl-2 was amplified by PCR using the flanking outer primers 5′-AGGgaattcATGGACGAGGACGTTTTGCC-3′ and 5′-AAAggatcc TTATCTCCTGCTCATCGCGA-3′ (lowercase letters denote restriction enzyme recognition sites) and cloned into pGEM-T Easy (Promega), which contains single 3′-T overhangs at the insertion site. The KS-Bcl-2 inserts were released by digestion of the resulting plasmid with EcoRI and BamHI and ligated into pAS2.1 (Clontech) and pEGFP-C2 (Clontech) to obtain a yeast expression plasmid and a GFP–KS-Bcl-2 mammalian expression plasmid, respectively. The pGEM-T Easy plasmid, which contains KS-Bcl-2, was also digested with EcoRI and ApaI, and the insert was subcloned into the mammalian expression plasmid pCMV-Tag2B (Stratagene), which allows N-terminal Flag tagging. To obtain an HA-tagged KS-Bcl-2 mammalian expression plasmid, pCMV-Tag2B-KS-Bcl-2 was digested with BamHI and ApaI, and the released insert was subcloned into pcDNA3-HA (Invitrogen).

To construct the deletion derivatives KS-Bcl-2Δ(1-17), KS-Bcl-2Δ(1-58), and KS-Bcl-2Δ(1-101), PCR was first performed using the outer sense primer 5′-A ACggatccATGGCCTGTGGATTAAACGAA-3′, 5′-AACggatccAGATTTCAC AGCACCACCGGT-3′, or 5′-AAAGGATCCTCCAACGAACCTCACCTGCG A-3′ and the outer antisense primer 5′-ACCgaattcGCGTTATCTCCTGCTCA TCGC-3′. The resulting products were digested with BamHI and EcoRI and cloned into pcDNA3-HA. These plasmids were then digested with BamHI and XbaI, allowing the subcloning of the inserts into the pEGFP-C1 expression plasmid. A GFP-tagged KS-Bcl-2Δ(37-42) mammalian expression plasmid was generated by two rounds of PCR. During the first round, the flanking outer primers described above, which contained EcoRI and BamHI sites, were used, together with overlapping inner sense and antisense primer pairs that contained the mutations. This round produced amplification products that overlapped at their 3′ and 5′ ends. A second round of amplification used these products as amplification templates with the outer primers described above. The deleted full-length PCR fragment of KS-Bcl-2 generated by the second round of PCR was inserted into pEGFP-C2. The inner oligonucleotide primers used were as follows: KS-Bcl-2Δ(37-42) inner sense, 5′-CTCAGCCCTATTTTAATGCGAG AC-3′, and inner antisense, 5′-GTCTCGCATTAAAATAGGGCTGAG-3′.

The pEF1-myc-PICT-1 mammalian expression vector (26) and the pSilencer 3.1 H1-hygro vector, encoding small hairpin RNA (shRNA) that targets PICT-1, were kindly provided by T. Maehama (Tokyo Metropolitan University, Tokyo, Japan) (27). Expression plasmids containing myc-tagged C-terminal PICT-1 deletion mutants were constructed using the full-length PICT-1 plasmid as a template for PCR with the antisense primer 5′-AAAtctagaATTCGCCAGCTCCG CCAGCCTCAG-3′, 5′ ACCtctagaATTCTGCTGCTCC GTCTTCTTCTC-3′, or 5′-AACtctagaATTCAGCCTTCGGGGCTTGTC-3′ and the sense primer 5′-CCGggtaccATGGAACAAAAACTCATCTCA-3′. The PCR products were then digested with KpnI and XbaI and cloned into the pEF1-myc-PICT-1 plasmid. N-terminal truncations of PICT-1 were obtained by PCR using the sense primer 5′-AAAggtaccATGGAACAAAAACTCATCTCAGAAGAAGATCTG CGGCGGCGGGAGAAG-3′ or 5′-AAAggtaccATGGAACAAAAACTCATC TCAGAAGAAGATCTGGCCGAGGTCTGTCCC-3′, together with the antisense primer 5′-AACtctagaGCAGCTACAACTGGATCTCA-3′. The PCR products were digested with KpnI and XbaI and cloned as described above. All cloned PCR products were verified by sequencing them.

The HA-ORF35 expression plasmid was previously described (23), GFP-huBcl-2 was kindly provided by L. Sherman (Tel Aviv University, Tel Aviv, Israel), and GFP-fibrillarin and GFP-tubulin expression plasmids were kindly provided by Y. Shav-Tal (Bar Ilan University, Israel). The GFP-ICP0 expression plasmid was kindly provided by R. Everett (MRC Virology Unit, Institute of Virology, Glasgow, Scotland).

Yeast two-hybrid screen. To identify proteins that interact with KS-Bcl-2, we employed the Matchmaker yeast two-hybrid screening system (Clontech). *Saccharomyces cerevisiae* strain AH109 harboring pAS2.1-KS-Bcl-2 was mated with the yeast strain Y187 pretransformed with a human bone marrow cDNA library on pACT2-AD according to the manufacturer's protocol. Diploid yeast clones were initially subjected to histidine nutritional selection on synthetic dropout (SD) plates lacking histidine, leucine, and tryptophan in the presence of 2.5 mM 3-amino-1,2,4-triazole. Positive clones from the first screening were then further subjected to adenine nutritional selection and β-galactosidase (β-Gal) assay according to Clontech Yeast Handbook protocols. Plasmid DNAs were prepared from colonies that activated all three yeast reporter genes (HIS3, ADE2, and LacZ), and were transformed into *Escherichia coli* HB101 and sequenced. Interactions were confirmed using a bait plasmid KS-Bcl-2 pretransformed AH109 yeast strain that was transformed with positive prey plasmids; these yeasts then underwent nutritional selection and were assayed for β-galactosidase activity. Simian virus 40 (SV40) large T-antigen and KSHV ORF45 fused to the GAL4 binding domain were used as controls.

Cell culture and transfection. Human epithelial kidney 293T (HEK-293T) cells and cervical cancer HeLa cells were grown in Dulbecco's modified Eagle's medium (DMEM) supplemented with 10% fetal calf serum (FCS) (Biological Industries, Kibbutz Beit Haemek, Israel) and antibiotics. KSHV-infected BCBL-1 cells were cultured in RPMI 1640 medium supplemented as described above. DNA transfections into 293T cells employed the calcium phosphate precipitation method or the TransIT-LT1 reagent (Mirus Bio LLC), while transfections into HeLa and BCBL-1 cells were performed using Lipofectamine 2000 (Invitrogen, Carlsbad, CA). In all cases, the total amount of DNA was equalized by the addition of control plasmids.

Western blot analysis. Cells were washed twice in cold phosphate-buffered saline (PBS), suspended in RIPA lysis buffer, and incubated on ice for 30 min. Then, cell debris was removed by centrifugation at 12,000 × *g* for 15 min at 4°C. Protein lysates were resolved by SDS-PAGE and transferred to nitrocellulose membranes (Schleicher & Schuell). The protein contents of different samples were verified to be similar by Ponceau S staining. The nitrocellulose membranes were blocked with 5% dry milk in Tris-buffered saline (TBS) and subsequently incubated with primary antibody. Specific reactive bands were detected using goat anti-rabbit IgG or goat anti-mouse conjugated to horseradish peroxidase. Immunoreactive bands were visualized using a enhanced chemiluminescence (ECL) Western blotting detection kit (Amersham, Arlington Heights, IL).

Immunoprecipitation assays. Transfected 293T cells were lysed in buffer containing 50 mM HEPES (pH 7.5), 150 mM NaCl, 1% Triton X-100, 10% glycerol, 1 mM EDTA (pH 8.0), 1 mM EGTA (pH 8.0), 1.5 mM $MgCl_2$, and protease inhibitor cocktail (Complete; Boehringer). Cell extracts were clarified by centrifugation at 14,000 × *g* for 5 min, and the resulting supernatant was incubated overnight at 4°C with anti-HA, anti-GFP, or anti-myc and then with protein A/G plus agarose beads (Santa Cruz Biotechnology). After intensive washing and centrifugation, immune complexes were separated by SDS-PAGE and probed by Western blotting.

Immunofluorescence microscopy. Cells were seeded on coverslips prior to transfection. At 24 h posttransfection, the cells were washed with PBS and fixed by incubation in 4% formaldehyde for 20 min at room temperature. The cells were then washed twice in PBS and permeabilized in PBS containing 0.1% Triton ×100 and 1% bovine serum albumin (BSA) at room temperature for 30

min. The cells were then probed with primary antibody at 4°C, and rhodamine red-conjugated secondary antibodies were applied for detection. To stain the nuclei, the cells were incubated for 30 min with 0.05 μg/ml Hoechst dye (Sigma). Chloromethyl-X-rosamine (MitoTracker Red) was used according to the manufacturers' instructions (Molecular Probes). Cells were examined and photographed under a confocal laser scanning microscope (Zeiss LSM 510 META).

Viability assays. For cell and nuclear morphology examination, HEK-293T cells (5×10^4) were cultured in 24-well plates and grown on glass coverslips. Transfections were carried out using the calcium phosphate precipitation method. The cells were cotransfected with a GFP marker plasmid (0.05 μg), and vectors expressing test proteins [0.1 μg BAX, 0.2 μg KS-Bcl-2, 0.2 μg myc–PICT-1, or 0.2 μg myc–PICT-1Δ(342-478)]. The total amount of plasmid DNA used in each transfection was normalized to 0.55 μg by adding empty pcDNA3 vector DNA. Twenty-four hours later, the cells on the coverslips were fixed and permeabilized, and the nuclei were stained as described above. The cell viability of blinded samples was determined by counting the number of GFP-positive cells in 15 independent fields and scoring for normal versus apoptotic morphology using an AxioImagerZ1 fluorescence microscope (Zeiss). The viability was expressed as relative units, with the BAX-transfected cells defined as 100. For the annexin V-propidium iodide (PI) staining assay, HEK-293T cells (1×10^5) were cultured in 12-well plates and transfected by using the TransIT-LT1 reagent (Mirus Bio LLC). The cells were transfected with 0.2 μg BAX, 0.6 μg KS-Bcl-2, 0.4 μg myc–PICT-1 wild type and myc–PICT-1Δ(342-478) in the indicated combinations, and the total amount of DNA was equalized by the addition of control empty plasmid. Twenty hours later, adherent and floating cells were collected, and an annexin V-fluorescein isothiocyanate (FITC)/PI assay was performed according to the manufacturer's instructions (Mebcyto apoptosis kit; MBL). Similarly, HEK-293T cells were transfected with 0.175 μg of *lacZ* reporter plasmid, together with plasmids coding for the indicated proteins (0.25 μg BAX, 0.4 μg KS-Bcl-2, or 0.3 μg myc–PICT-1). The total amount of plasmids transfected was held constant at 1.125 μg by using empty vectors. Cell lysates were prepared 24 h after transfection, and β-galactosidase activity was measured using the Promega β-Galactosidase Enzyme Assay System kit, according to the manufacturer's instructions. The β-Gal activity was expressed as relative units, with the control cell activity defined as 100%.

RESULTS

Identification of PICT-1 as a KS-Bcl-2 target of interaction in yeast. To identify protein partners of KS-Bcl-2, we performed a yeast two-hybrid screen using full-length KS-Bcl-2 as bait and a human bone marrow cDNA library as prey. Among the 1×10^6 independent clones screened, we isolated two positive clones that corresponded to amino acids (aa) 2 to 478 and 136 to 478 of PICT-1/GLTSCR2. To corroborate the specificity of the KS-Bcl-2 and PICT-1 interaction, we transformed the PICT-1-containing plasmids into AH109 yeast pretransformed with KS-Bcl-2. The two-hybrid interaction assays showed that coexpression of KS-Bcl-2 and PICT-1 resulted in activation of the HIS3, ADE, and *lacZ* reporter genes, as indicated by growth of the transformants on nutritionally deficient media and the formation of blue colonies on colony lift filters in the presence of 5-bromo-4-chloro-3-indolyl-β-D-galactopyranoside (X-Gal). Control experiments, including KS-Bcl-2 alone or together with p53 fused to the GAL4 activation domain, and coexpression of PICT-1, together with SV40 large T-antigen or KS ORF45 (an irrelevant KSHV-derived gene) fused to the GAL4-binding domain, failed to activate the reporter genes, whereas activation of the reporter genes was evident in the positive control including the combination of SV40 large T-antigen and p53 (Table 1). These results indicate that PICT-1 interacts specifically with KS-Bcl-2 in yeast.

KS-Bcl-2 associates physically with PICT-1 in mammalian cells. To confirm our two-hybrid screen results in mammalian cells, we performed coimmunoprecipitation experiments. An HA-tagged KS-Bcl-2 expression construct was transiently transfected into 293T cells, together with the myc–PICT-1 expression construct or a control pcDNA3-myc plasmid. In addition, cells were cotransfected with the myc–PICT-1 expression construct and a plasmid expressing KSHV ORF35 tagged with HA. Expression of the target proteins was detected by Western blotting (Fig. 1A, Input), and lysates of transfectants were subjected to immunoprecipitation with monoclonal anti-HA antibody. KS-Bcl-2 immunoprecipitated from 293T cell lysates by anti-HA antibody and was positive for interaction with the myc–PICT-1 protein, whereas PICT-1 could not be detected within the immunoprecipitation control (Fig. 1A, IP). This interaction was also observed when endogenous PICT-1 was coimmunoprecipitated with GFP-KS-Bcl-2 (Fig. 1B). Of note, as previously reported (39), although we detected high levels of mRNA encoding KS-Bcl-2, we failed to detect KS-Bcl-2 protein in cells experimentally infected with KSHV, and therefore, our study was carried out by using ectopically expressed KS-Bcl-2. These results support the yeast-two hybrid findings, further suggesting that KS-Bcl-2 interacts with PICT-1 in mammalian cells.

TABLE 1. Interaction of KS-Bcl-2 and PICT-1 in the yeast two-hybrid system[a]

GAL4-binding plasmid	β-Galactosidase and HIS reactions with activation domain plasmid:			
	None	p53	PICT-1(2–478)	PICT-1(136–478)
KS-Bcl-2	−	−	+	+
SV40 large T antigen	−	+	−	−
KS-ORF45	−	−	−	−

[a] Transformants coexpressing KS-Bcl-2 and the indicated activation domain fusion proteins were used to confirm the findings obtained using the yeast two-hybrid screen. Empty, p53, SV40 large T antigen, and KS-ORF45 fusion proteins were used as negative and positive controls. Two variants, corresponding to amino acids 2 to 478 and 136 to 478 of PICT-1/GLTSCR2, were included. Interaction (+) or lack of interaction (−) are indicated with respect to β-galactosidase activity and auxotrophic selective marker expression (HIS).

PICT-1 induces nucleolar localization of KS-Bcl-2. Nonionic detergents have been reported to induce artifactual *in vitro* dimerization and coimmunoprecipitation among members of the Bcl-2 family (17). Therefore, we applied indirect confocal immunofluorescence microscopy to examine the localization of KS-Bcl-2 and PICT-1 in transfected cells. Upon transfection of a GFP-tagged KS-Bcl-2 expression vector into 293T cells, we noticed that KS-Bcl-2 was located mostly at the mitochondrial membranes. A small fraction of the KS-Bcl-2 was detected in the nucleoli (Fig. 2). However, PICT-1 was predominantly detected in the nucleoli following transfection of a myc-tagged PICT-1 expression vector (Fig. 2). Endogenous PICT-1, detected with anti-PICT-1 antibodies, was also identified in the nucleoli, though it appeared in a punctate pattern (Fig. 2). To further verify the nucleolar localization of PICT-1, we coexpressed myc–PICT-1 with GFP-fibrillarin, a known rRNA-processing protein localized at the nucleolus. As shown in Fig. 2, although the precise localizations and distributions of myc–PICT-1 and GFP-fibrillarin were different, both were localized to the nucleoli. This finding is consistent with previous studies of the human nucleolus proteome, in which PICT-1 was identified among nucleolar proteins (1, 32).

To determine whether PICT-1 and KS-Bcl-2 colocalize in cells, we cotransfected myc-tagged PICT-1 and GFP-tagged

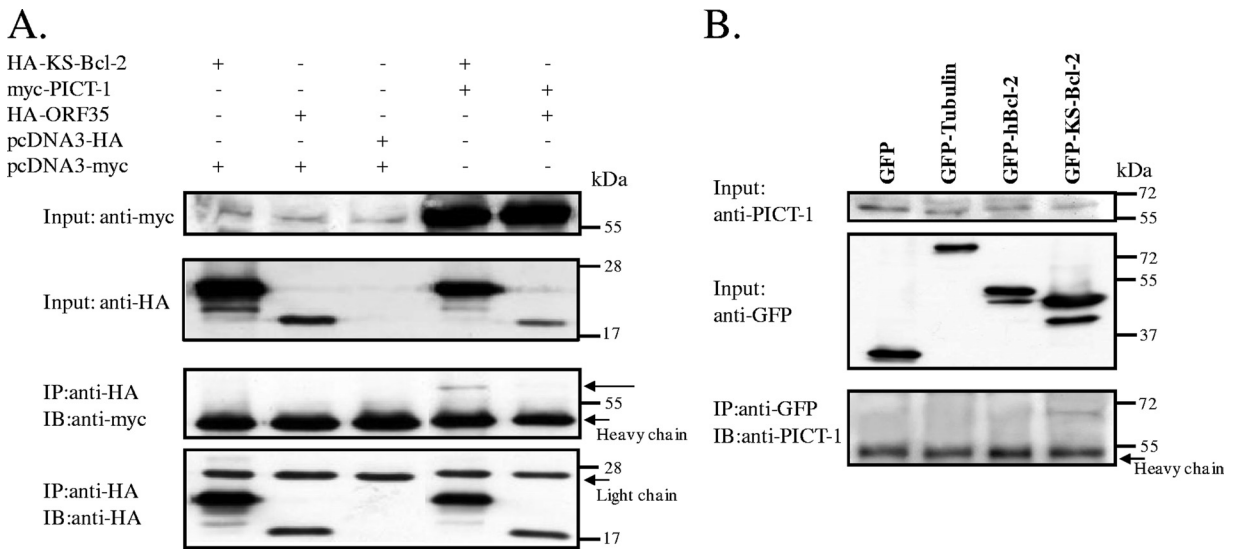

FIG. 1. KS-Bcl-2 physically associates with PICT-1 in 293T cells. (A) To detect the association between PICT-1 and KS-Bcl-2, expression vectors containing HA–KS-Bcl-2 and myc–PICT-1 were transfected into 293T cells. Cells transfected with the HA–KS-Bcl-2 expression vector, together with control empty vector (pcDNA-myc), were used as negative controls. myc–PICT-1 cotransfected with HA-tagged ORF35 (HA-ORF35) served as an additional control. After 24 h, whole-cell extracts were prepared and 30-μg aliquots were analyzed for protein expression with antibodies to HA and myc (Input). Next, 400 μg of the lysates was subjected to immunoprecipitation (IP) with anti-HA, followed by sequential Western blotting (IB) with anti-myc and anti-HA antibodies. As indicated by the arrows, myc–PICT-1 coprecipitated with HA-KS-Bcl-2 but not with the unrelated protein HA-ORF35. (B) Similarly, GFP, GFP-tubulin, GFP–hBcl-2, and GFP–KS-Bcl-2 expression vectors were transfected into 293T cells. After 24 h, whole-cell extracts were prepared and analyzed for protein expression with antibodies to PICT-1 and GFP to detect the endogenous and exogenous proteins, respectively (Input). Whole-cell lysates were then immunoprecipitated with anti-GFP and immunoblotted with anti-PICT-1 antibody.

KS-Bcl-2 expression vectors into 293T and HeLa cells and determined the distribution of these proteins by confocal laser scanning microscopy. As shown, ectopic expression of PICT-1 resulted in a large increase in the nucleolar fraction of KS-Bcl-2, and only a minor fraction of KS-Bcl-2 remained in the cytoplasm. In contrast, expression of PICT-1 together with GFP or GFP-tubulin did not alter their cellular distribution. Furthermore, nucleolar localization of GFP-tagged human Bcl-2 (GFP–hu-Bcl-2) was not observed when it was coexpressed with PICT-1 (Fig. 3A and B), supporting the exclusiveness of our observation. Similar results were obtained in HeLa cells (data not shown) and in KSHV-infected BCBL-1 cells (Fig. 3C). These results indicate that GFP by itself does not influence the distribution of its fusion partners and validates the authenticity of the interaction between KS-Bcl-2 and PICT-1. Furthermore, these results implicate PICT-1 as the partner that participates in the recruitment of KS-Bcl-2 to the nucleolus.

Knockdown of endogenous PICT-1 abolishes the nucleolar localization of KS-Bcl-2. Our findings suggested that PICT-1 is involved in the nucleolar targeting of KS-Bcl-2. In order to determine whether PICT-1 is necessary for the nucleolar localization of KS-Bcl-2, we inhibited PICT-1 expression with a gene-specific shRNA. As shown in Fig. 4, the nucleolar localization of KS-Bcl-2 was abrogated following the knockdown of PICT-1. Similar results were obtained in HeLa cells (not shown). Thus, these experiments established that PICT-1 is essential for the nucleolar targeting of KS-Bcl-2.

Identification of PICT-1 sequences required for its nucleolar targeting and for the interaction with KS-Bcl-2. Yim and colleagues recently identified "a discrete globular expression pattern" of an enhanced GFP (EGFP)-tagged PICT-1 protein (40). By using a series of PICT-1 truncations, the group mapped two putative nuclear localization signals (NLS) at the amino and carboxy termini of PICT-1, while a distinct carboxy-terminal sequence (aa 347 to 478) was found to be crucial for the globular localization pattern. To map the interaction site between PICT-1 and KS-Bcl-2, we generated a series of PICT-1 deletion mutants and examined their cellular localization and their impact on the cellular distribution of KS-Bcl-2. As shown in Fig. 5A, mutants with deletion of the carboxy terminus of PICT-1 [PICT-1Δ(407-478) and PICT-1Δ(387-478)] and mutants with deletion of amino acids 1 to 341 [PICT-1Δ(1-321) and PICT-1Δ(1-341)] were still localized to the nucleoli and were capable of inducing the nucleolar accumulation of KS-Bcl-2 as well. In contrast, PICT-1Δ(342-478) lost localization to the nucleoli, presented a diffused nuclear staining pattern, and failed to induce the nucleolar accumulation of KS-Bcl-2. These results suggest that amino acids 342 to 386 are crucial for the nucleolar targeting of PICT-1. Furthermore, since PICT-1Δ(1-341) and PICT-1Δ(387-478) targeted KS-Bcl-2 to the nucleoli, whereas PICT-1Δ(342-478) failed to alter the cellular distribution of KS-Bcl-2, it appears that the same amino acids (342 to 386) are also essential for the interaction between PICT-1 and KS-Bcl-2. Coimmunoprecipitation assays using protein extracts from cells expressing GFP–KS-Bcl-2 and full-length or truncated PICT-1 confirmed this conclusion (Fig. 5B).

Identification of the KS-Bcl-2 sequences required for binding with PICT-1. To define the region of KS-Bcl-2 required for the interaction with PICT-1, we first generated a series of deletion mutants of GFP-tagged KS-Bcl-2 and examined their localization upon ectopic expression of PICT-1. The results revealed that KS-Bcl-2Δ(1-17) retained little ability to accu-

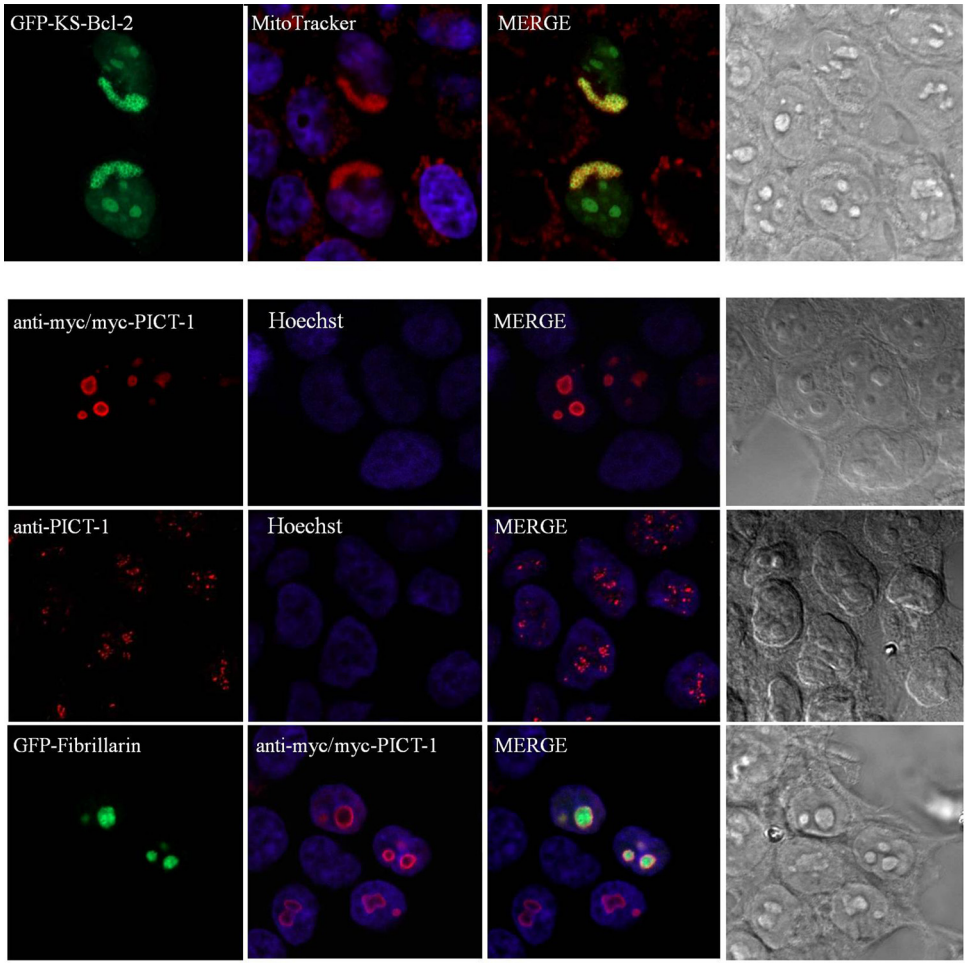

FIG. 2. Cellular localization of KS-Bcl-2 and PICT-1. 293T cells were transfected with the indicated expression plasmids. Mitochondrial localization of KS-Bcl-2 was confirmed with MitoTracker. Ectopically expressed myc–PICT-1 was detected by anti-myc, while endogenous expression was identified with anti-PICT-1 antibody. GFP-fibrillarin was used as a marker for nucleoli. The corresponding staining of nuclear DNA by Hoechst and differential interference contrast (DIC) imaging is also displayed.

mulate in the nucleoli upon cotransfection of PICT-1, though this was evident in only a fraction of the cells. In the majority of the cells, KS-Bcl-2Δ(1-17) remained cytosolic (Fig. 6A). KS-Bcl-2Δ(1-58) and KS-Bcl-2Δ(1-94) truncation mutants failed to accumulate in the nucleoli when expressed alone or together with ectopic expression of PICT-1. In accordance with this, KS-Bcl-2Δ(1-58) and KS-Bcl-2Δ(1-94) failed to coimmunoprecipitate with PICT-1, whereas full-length KS-Bcl-2 and the HA–KS-Bcl-2Δ(1-17) mutant coimmunoprecipitated with PICT-1 (Fig. 6B). These results suggest that the critical residues in KS-Bcl-2 for the binding of PICT-1 map in its BH3 domain, between amino acids 18 and 58.

PICT-1 has been found to interact with the phosphatase and tensin homologue deleted on chromosome 10 (PTEN) (26). The region that appears to be responsible for the interaction between PICT-1 and PTEN is known as a "hot spot" for C-terminal tumor-associated missense mutations. Moreover, the C-terminal mutants F341V, V343E, and L345Q of PTEN, identified in certain tumors, completely lose their binding to PICT-1. PICT-1, initially referred to as p60, was also shown to interact with ICP0, encoded by herpes simplex virus type 1 (HSV-1). This interaction was mapped to amino acids 111 to 241 of ICP0 (6). By using BLAST analysis, we identified a short region of amino acid sequence homology between the putative PICT-1 interaction domains of PTEN and ICP0 and amino acids 34 to 42 of KS-Bcl-2, providing a clue to the precise site of interaction (Fig. 6C). Based on this finding, we constructed a GFP–KS-Bcl-2 mutant in which we deleted 6 amino acids that were found to be relatively conserved among the three reported interacting proteins of PICT-1 (Fig. 6D). As shown in Fig. 6E, KS-Bcl-2Δ(37-42) failed to accumulate in the nucleoli upon overexpression of PICT-1. Moreover, this deleted KS-Bcl-2 mutant was not detected in the nucleoli when expressed alone. Furthermore, KS-Bcl-2Δ(37-42) failed to form a physical interaction with PICT-1, as determined by coimmunoprecipitation (Fig. 6F). Taken together, these experiments confirmed that PICT-1 interacts with a conserved binding motif, located at amino acids 37 to 42 of KS-Bcl-2, which is partially shared with two other interacting proteins. The impaired nucleolar targeting of the KS-Bcl-2Δ(1-17) mutant suggests that regions outside the conserved binding domain may assist in this interaction.

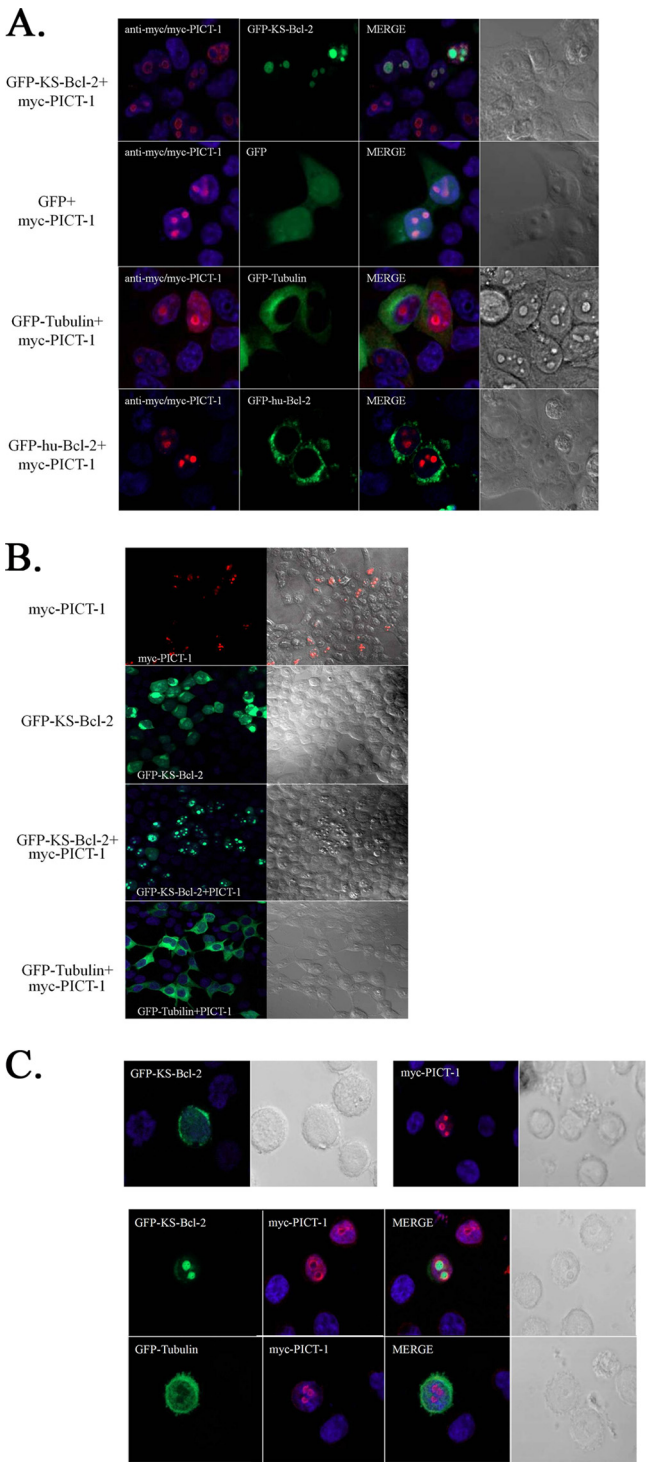

FIG. 3. KS-Bcl-2 accumulates in the nucleoli when coexpressed with PICT-1. (A) 293T cells were transfected with the indicated expression plasmids. Overexpression of PICT-1 increased the nucleolar localization of KS-Bcl-2 but failed to affect the cellular localization of GFP, GFP-tubulin, or GFP–hu-Bcl-2. Hoechst staining was used to visualize cell nuclei, and DIC images were used to demonstrate the morphology of the cells. (B) Lower magnification showing the extensive and selective effect of the expression of PICT-1 on the cellular localization of GFP–KS-Bcl-2 in transfected 293T cells. (C) BCBL-1 cells were transfected with the indicated expression plasmids and visualized as described above.

PICT-1 inhibits the antiapoptotic activity of KS-Bcl-2. To gain insight into the functional significance of the interaction between KS-Bcl-2 and PICT-1, we investigated the effect of PICT-1 on the antiapoptotic activity of KS-Bcl-2. One of the functions of KS-Bcl-2 is to inhibit cell death induced by BAX (4, 31). This activity has been suggested to take place in the mitochondria. To determine the impact of PICT-1 on the antiapoptotic activity of KS-Bcl-2, we transiently cotransfected HEK-293T cells with plasmids encoding GFP, BAX, and KS-Bcl-2, together with myc–PICT-1 or PICT-1Δ(342-478). At 24 h, transfected cells, identified by the expression of GFP, were assessed and scored as alive or dead based on their morphology. As shown in Fig. 7A, KS-Bcl-2-transfected cells exhibited a relatively high survival rate when coexpressed with BAX. This result is consistent with previous studies showing that KS-Bcl-2 confers protection against BAX-induced cell death (4, 31). Expression of PICT-1 or PICT-1Δ(342-478) alone did not enhance or suppress the cell-killing function of BAX. However, expression of PICT-1 repressed the protection against BAX-induced cell death provided by KS-Bcl-2. Interestingly, increased survival was evident when BAX was coexpressed with KS-Bcl-2 and PICT-1Δ(342-478), which does not interact with KS-Bcl-2. This suggests that PICT-1Δ(342-478) might inhibit endogenous PICT-1 or may have unique prosurvival properties. A similar pattern was evident when the percentage of apoptotic cells was evaluated by using the annexin V/PI assay (Fig. 7B) and when the β-galactosidase activity assay was carried out using protein extracts from cells transfected with the effector expression plasmids, together with a *lacZ* reporter plasmid (Fig. 7C). Of note, transfection of the different plasmids alone or cotransfection of KS-Bcl-2 together with PICT-1 or PICT-1Δ(342-478) expression plasmids did not affect cell viability, as determined by the different assays at 20 and 24 h posttransfection (data not shown). These results suggest that PICT-1 inhibits the antiapoptotic activity of KS-Bcl-2 through its sequestration from the mitochondria to the nucleoli. Taken together, our findings suggest a correlation between nucleolar targeting of KS-Bcl-2 by PICT-1 and reduction of the antiapoptotic activity of KS-Bcl-2.

DISCUSSION

In this study, we identified a cellular protein, PICT-1, encoded by a candidate glioma tumor suppressor gene, GLTSCR2, which interacts specifically with KS-Bcl-2 in a yeast two-hybrid system. This interaction was also demonstrated using coimmunoprecipitation and was confirmed by confocal laser scanning microscopy of labeled proteins. In line with our findings, PICT-1 was previously localized within the nucleoli of human cells (1, 32). PICT-1 shares homology with the yeast 60S ribosomal protein Nop53p (14). The exact cellular function of PICT-1 is still largely undefined. PICT-1 was initially identified as a 60-kDa protein (p60) that interacts with HSV-1 ICP0 and ICP22 (6). The interaction domain of KS-Bcl-2 with PICT-1 shares homology with a few ICP0 residues that were previously mapped to form the interaction site with p60. In fact, we noticed the targeting of ICP0 to the nucleoli when coexpressed with PICT-1 (data not shown). However, although nucleolar localization of ICP0 has been previously reported to

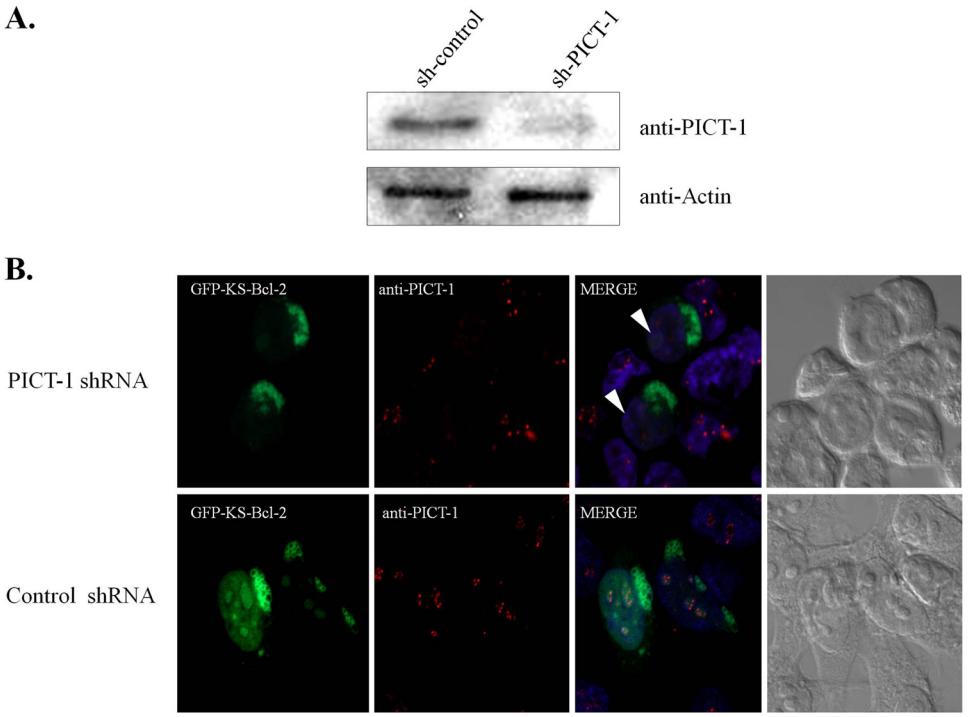

FIG. 4. Knockdown of endogenous PICT-1 aborogates the nucleolar localization of KS-Bcl-2. (A) pSilencer 3.1 H1-hygro plasmids encoding shRNA targeting PICT-1 or control shRNA were transfected into 293T cells, and 24 h after transfection, 100 μg/ml hygomycin was added. After 4 days, a GFP–KS-Bcl-2 expression vector was transfected, and protein cell extracts were prepared and assayed with antibodies to PICT-1 to confirm knockdown; anti-actin was included as a loading control. (B) In parallel, cells were fixed, and slides were prepared and viewed as described for panel A. The arrowheads indicate cells in which the expression of PICT-1 was knocked down and KS-Bcl-2 was not found the nucleoli.

occur during HSV-1 infection (24), the functional significance of these findings has not been elucidated.

The GLTSCR2 gene, which encodes PICT-1, is located within a common tumor suppressor region in chromosome 19q, which was originally identified in gliomas (35). Its tumor-related function is further supported by decreased expression and genetic alterations of GLTSCR2 in human neuroblastomas and glioblastomas (20, 28). Several lines of recent evidence support the involvement of PICT-1 in the suppression of tumor development and proliferation. PICT-1 physically interacts with the carboxy terminus region of the tumor suppressor PTEN, and appears to regulate its phosphorylation and to increase its stability (26). PTEN is a lipid phosphatase that dephosphorylates phosphatidylinositol-3,4,5 triphosphate (PIP3) and opposes phosphatidylinositol 3-kinase (PI3K) signaling (36). This important gene is frequently inactivated in multiple human tumors. Knockdown of PICT-1 induces anchorage-independent tumor cell growth and decreases susceptibility to apoptotic death stimuli (28, 40). In addition, caspase- and mitochondrion-independent cell death is induced following PICT-1 overexpression. Both phenomena are PTEN dependent (28, 40). The involvement of PICT-1 in maintaining PTEN stability suggests that loss-of-function mutations in PICT-1 may result in the reduction of cellular PTEN and may subsequently dysregulate PI3K-mediated signaling. Much remains unknown about the molecular pathways involving PICT-1 in association with PTEN and about regulating cell fate in general.

PICT-1 has two nuclear localization signals and a single nucleolar localization signal around residues 342 to 386, which was mapped in the present study (Fig. 5). This region also includes the KS-Bcl-2-interacting domain. Functional studies showed that wild-type PICT-1, which targets KS-Bcl-2 to the nucleoli, decreased the antiapoptotic activity of KS-Bcl-2, but the protein itself did not increase cell death. However, the PICT-1Δ(342-478) mutant was defective in targeting KS-Bcl-2 to the nucleoli and also failed to reduce the antiapoptotic activity of KS-Bcl-2. These results suggest that repression of the antiapoptotic activity of KS-Bcl-2 is dependent on its increased cellular targeting to the nucleoli. Mapping of the PICT-1-binding domain of KS-Bcl-2 showed that aa 37 to 42, included in the BH3 domain, are critical for the interaction with PICT-1. This domain is partially shared with the putative PICT-1-interacting domains of ICP0 and PTEN, suggesting a conserved interaction domain with PICT-1. Previous studies implicated the BH3 domain in the cytotoxic activity of proapoptotic Bcl-2 family members and in the homo- and heterodimerization between Bcl-2 family members. Therefore, the binding of PICT-1 through the BH3 domain may influence other potential protein interactions. However, in contrast to KS-Bcl-2, human Bcl-2, which shares limited sequence homology with KS-Bcl-2, was not targeted to the nucleoli by PICT-1. Hence, alternative mechanisms, such as different posttranslational modifications and protein interactions, may modulate the abilities of KS-Bcl-2 and other Bcl-2 family members to mediate their unique functions.

Accumulating evidence indicates that proteins of the Bcl-2 family fulfill their pro- or antiapoptotic roles largely through their effects on the mitochondria (15, 37). Mitochondria play a

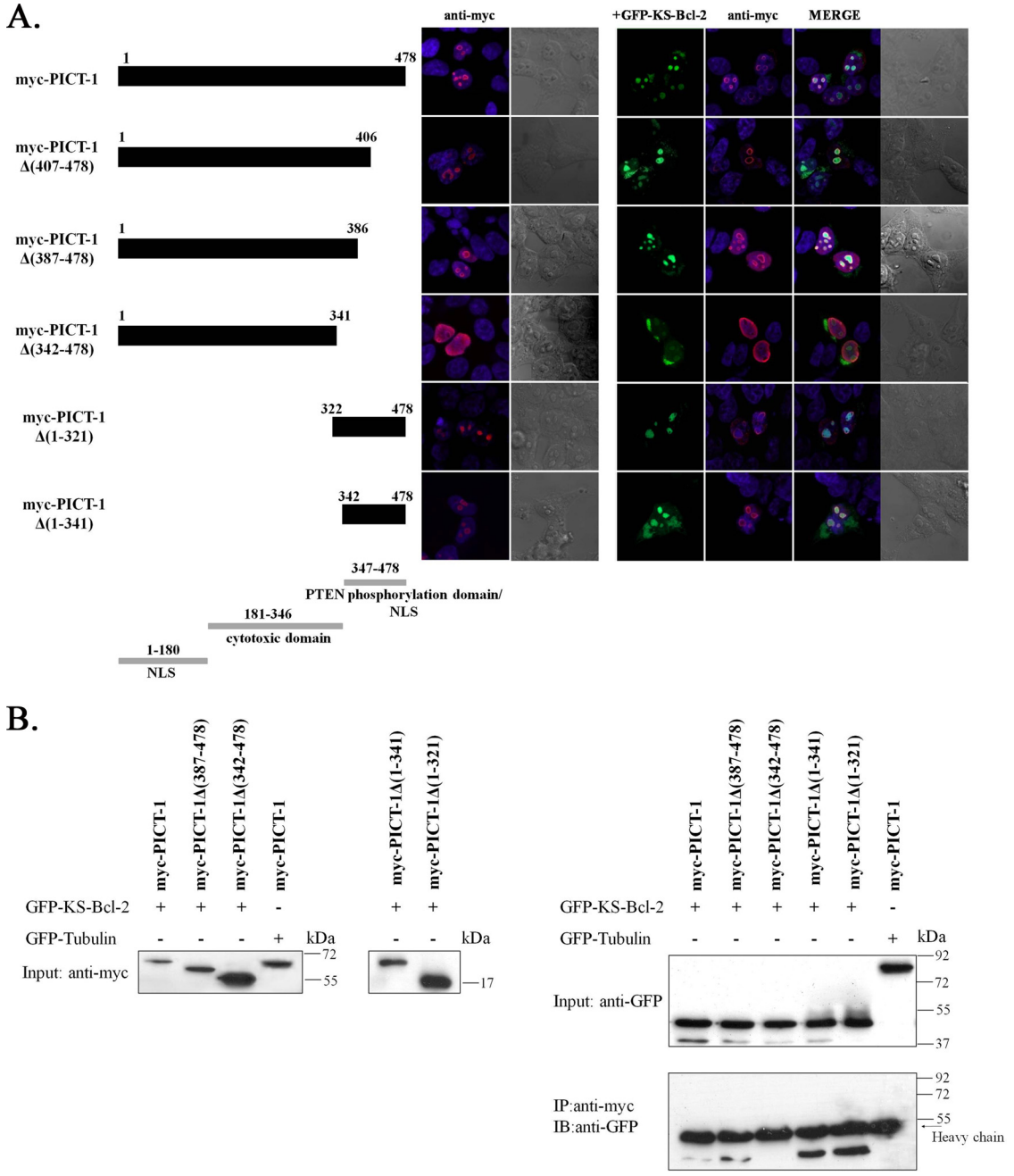

FIG. 5. Mapping the nucleolar localization signal of PICT-1 and the requirements for KS-Bcl-2 interaction. (A) Schematic representations of wild-type PICT-1 and its deletion mutants used in the mapping experiments; the boundary amino acids are numbered. The results of previously published functional mapping of PICT-1 (40) are shown in gray. 293T cells were transfected with the indicated myc–PICT-1 expression plasmid alone or with GFP–KS-Bcl-2, and the subcellular localization of the respective deletion mutant proteins was determined by immunofluorescence after staining them with anti-myc antibody and Hoechst. (B) Western blots showing coprecipitation of full-length and truncated myc–PICT-1 and KS-Bcl-2. Extracts of 293T cells cotransfected with plasmids encoding KS-Bcl-2 and full-length myc–PICT-1 or the indicated PICT-1 deletion mutants were first examined for exogenous protein expression with anti-GFP and anti-myc antibodies. The expression of full-length and truncated myc–PICT-1 is presented in two separate gels of 12% and 15% PAGE displaying their size differences (Input). Whole-cell extracts were immunoprecipitated with anti-myc antibody, and the presence of KS-Bcl-2 in the precipitates was examined by probing with anti-GFP antibody. GFP-tubulin was used as a negative control.

pivotal role in the apoptotic signaling pathway by releasing factors into the cytoplasm that in turn elicit a caspase cascade and induce apoptosis. KS-Bcl-2, a structural and functional viral homologue of the cellular Bcl-2 protein, has been shown to inhibit the mitochondrial events that lead to caspase activation and apoptosis (13). Like KS-Bcl-2, several apoptotic regulators, including Bcl-2 family members, are found in the nucleus, and some have been shown to acquire unique activities

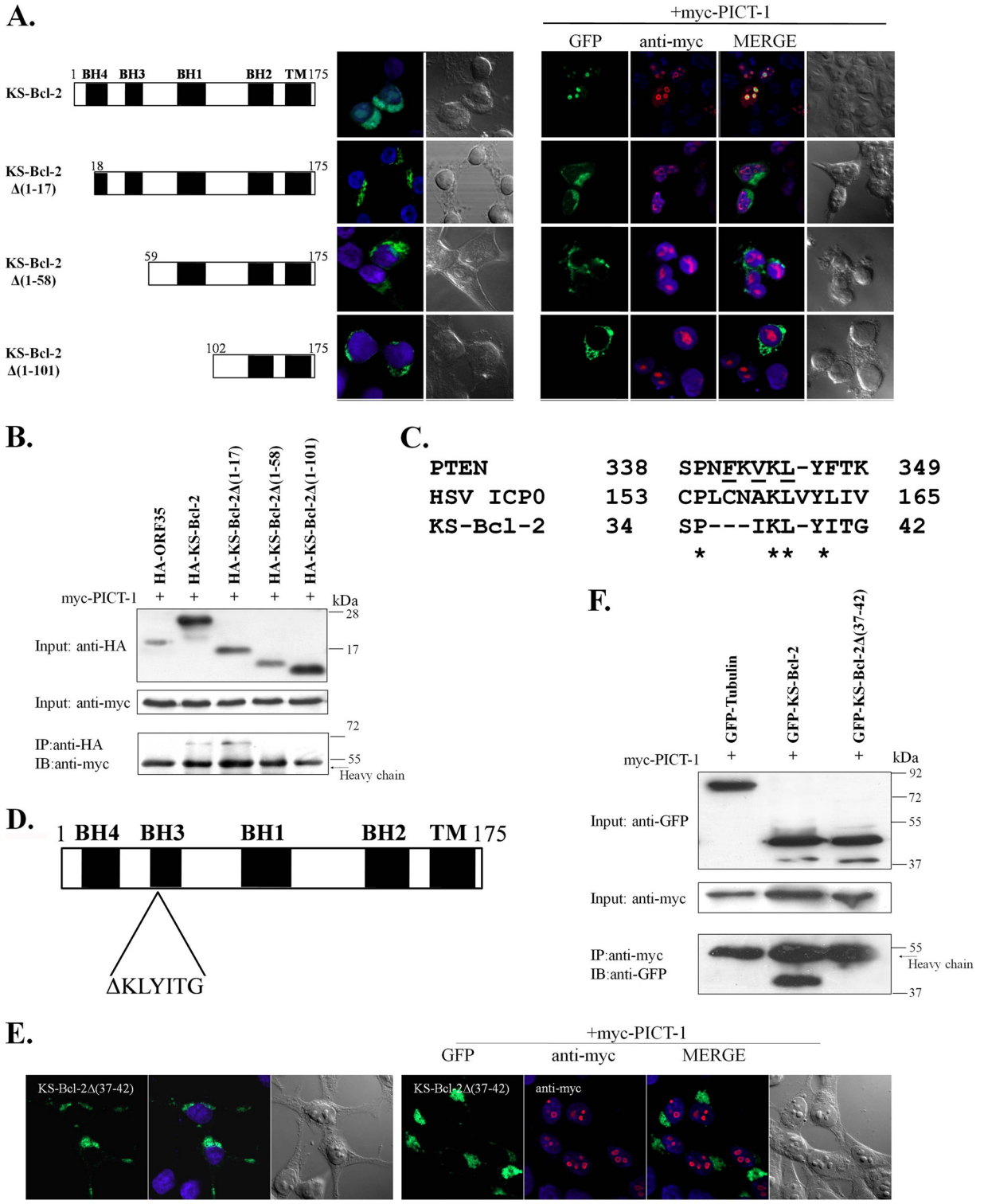

FIG. 6. Mapping the binding domain of KS-Bcl-2 to PICT-1. (A) Schematic representations of wild-type KS-Bcl-2 and its deletion mutants used in the mapping experiments; the boundary amino acids are numbered. The locations of the BH-1 to -4 motifs and the transmembrane domain are indicated. 293T cells were transfected with the indicated GFP–KS-Bcl-2 expression plasmid alone or with myc–PICT-1, and the subcellular localization of the respective deletion mutant proteins was determined by immunofluorescence after staining them with anti-myc antibody and Hoechst. (B) Western blots showing coprecipitation of KS-Bcl-2 mutants and PICT-1. Extracts of 293T cells cotransfected with plasmids encoding PICT-1 and full-length KS-Bcl-2 or the indicated KS-Bcl-2 deletion mutants were first examined for exogenous protein expression with anti-HA and anti-myc antibodies (Input). Whole-cell extracts were then immunoprecipitated with anti-HA antibody, and the presence of PICT-1 in the precipitates was examined by probing with anti-myc antibody. (C) Alignment of potential PICT-1-binding motifs of PTEN, ICP0, and KS-Bcl-2. PTEN mutations that lost their binding to PICT-1 are underlined. (D and E) Schematic diagram of KS-Bcl-2Δ(37-42) (D) and its cellular localization when expressed alone or together with myc–PICT-1 (E). (F) Plasmids encoding myc–PICT-1 were cotransfected with GFP-tubulin, GFP–KS-Bcl-2, or GFP–KS-Bcl-2Δ(37-42) mutant into 293T cells, and exogenous protein expression was verified (Input). Whole-cell extracts were then immunoprecipitated with anti-myc antibody, and the presence of KS-Bcl-2 in the precipitates was examined by probing with anti-GFP antibody.

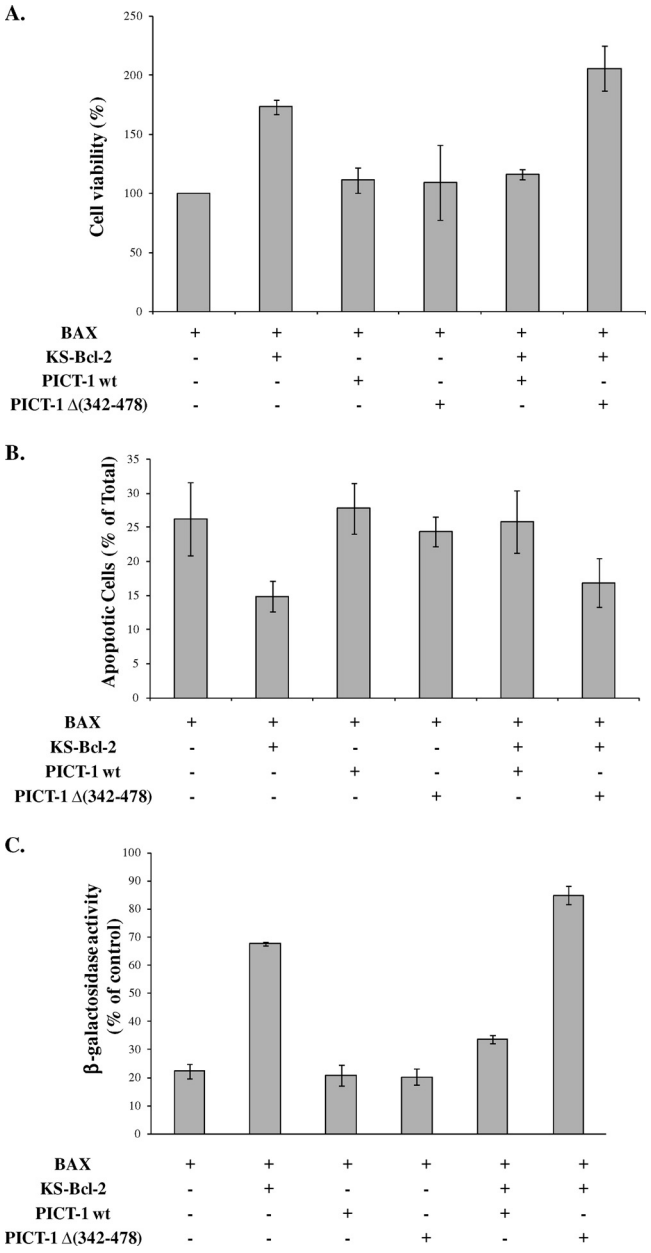

FIG. 7. PICT-1 reduces the antiapoptotic activity of KS-Bcl-2. (A) 293T cells were transfected with the indicated plasmids, together with GFP expression plasmid to mark the transfected cells. All samples received equal amounts of DNA. The viability of the cells was determined at 24 h posttransfection by scoring the percentage of transfected cells that were alive and/or nonapoptotic (>130 GFP-positive cells in 15 independent fields were counted blindly per sample). Means ± standard deviations of three independent experiments are shown. (B) 293T cells were cotransfected with the indicated expression vectors. Apoptosis was measured at 20 h posttransfection via flow cytometry by staining the cells with annexin V-FITC and PI. The data are presented as percentages of annexin V-positive cells and represent the means ± standard deviations of five experiments. (C) 293T cells were cotransfected with the indicated expression vectors, together with a vector for β-Gal. Cells were harvested 24 h posttransfection and assayed for β-Gal activity. The results shown are means ± standard deviations ($n = 3$) and are representative of three independent experiments. wt, wild type.

when targeted to this compartment (19, 33). Of note, Bcl-xL colocalizes and binds to cdk1 (cdc2) within the nucleoli at the G_2/M cell cycle checkpoint induced by DNA damage. This has been suggested to inhibit cdk1 kinase activity and to suppress potential apoptotic triggers induced by unscheduled cdk1 activation (34). Similarly, phosphorylated human Bcl-2 was found to colocalize with the nucleolar proteins Ki-67 and nucleolin in the nucleoli during prophase, and colocalization on the surfaces of mitotic chromosomes was observed during later mitotic stages (2). Collectively, these observations support an additional functional role for Bcl-2 proteins at the cell cycle checkpoint.

Nucleoli are membrane-free dynamic nuclear subdomains in which transcription and processing of rRNA and ribosome assembly take place (5). However, several nonribosomal proteins, including regulators of cell fate, such as HDM2, p14ARF, telomerase reverse transcriptase, and Bcl-2, were demonstrated to localize in this subnuclear compartment under certain conditions. This is consistent with additional processes that take place in the nucleolus, such as cell cycle control and the stress response. Here, we demonstrate the nucleolar localization of KS-Bcl-2 and suggest that its interaction with PICT-1 functions to sequester KS-Bcl-2 away from the mitochondria and to downregulate its antiapoptotic activity. This may represent an antiviral cellular response to inhibit the virus-encoded function of apoptosis inhibition. Nevertheless, nucleolar KS-Bcl-2 could interact in the nucleolus with a unique set of proteins that are involved in additional cellular processes, such as ribosome biogenesis and cell cycle core machinery. Moreover, KS-Bcl-2 may modify the function of PICT-1 and may participate in the modulation of pathways associated with the function of PTEN. Further characterization of the interaction between KS-Bcl-2 and PICT-1 may shed light on the functions of both proteins.

ACKNOWLEDGMENTS

This work was supported by grants from the Chief Scientist's Office of the Ministry of Health, Israel, and the Israel Science Foundation (grant no. 495/06).

REFERENCES

1. **Andersen, J. S., Y. W. Lam, A. K. Leung, S. E. Ong, C. E. Lyon, A. I. Lamond, and M. Mann.** 2005. Nucleolar proteome dynamics. Nature **433:**77–83.
2. **Barboule, N., I. Truchet, and A. Valette.** 2005. Localization of phosphorylated forms of Bcl-2 in mitosis: co-localization with Ki-67 and nucleolin in nuclear structures and on mitotic chromosomes. Cell Cycle **4:**590–596.
3. **Bellows, D. S., B. N. Chau, P. Lee, Y. Lazebnik, W. H. Burns, and J. M. Hardwick.** 2000. Antiapoptotic herpesvirus Bcl-2 homologs escape caspase-mediated conversion to proapoptotic proteins. J. Virol. **74:**5024–5031.
4. **Bellows, D. S., M. Howell, C. Pearson, S. A. Hazlewood, and J. M. Hardwick.** 2002. Epstein-Barr virus BALF1 is a BCL-2-like antagonist of the herpesvirus antiapoptotic BCL-2 proteins. J. Virol. **76:**2469–2479.
5. **Boisvert, F. M., S. van Koningsbruggen, J. Navascues, and A. I. Lamond.** 2007. The multifunctional nucleolus. Nat. Rev. Mol. Cell Biol. **8:**574–585.
6. **Bruni, R., B. Fineschi, W. O. Ogle, and B. Roizman.** 1999. A novel cellular protein, p60, interacting with both herpes simplex virus 1 regulatory proteins ICP22 and ICP0 is modified in a cell-type-specific manner and is recruited to the nucleus after infection. J. Virol. **73:**3810–3817.
7. **Chau, B. N., E. H. Cheng, D. A. Kerr, and J. M. Hardwick.** 2000. Aven, a novel inhibitor of caspase activation, binds Bcl-xL and Apaf-1. Mol. Cell **6:**31–40.
8. **Chen, Y. B., S. Y. Seo, D. G. Kirsch, T. T. Sheu, W. C. Cheng, and J. M. Hardwick.** 2006. Alternate functions of viral regulators of cell death. Cell Death Differ. **13:**1318–1324.
9. **Cheng, E. H., J. Nicholas, D. S. Bellows, G. S. Hayward, H. G. Guo, M. S. Reitz, and J. M. Hardwick.** 1997. A Bcl-2 homolog encoded by Kaposi sarcoma-associated virus, human herpesvirus 8, inhibits apoptosis but does

not heterodimerize with Bax or Bak. Proc. Natl. Acad. Sci. U. S. A. **94:**690–694.
10. **Cohen, A., D. G. Wolf, E. Guttman-Yassky, and R. Sarid.** 2005. Kaposi's sarcoma-associated herpesvirus: clinical, diagnostic, and epidemiological aspects. Crit. Rev. Clin. Lab. Sci. **42:**101–153.
11. **Cuconati, A., and E. White.** 2002. Viral homologs of BCL-2: role of apoptosis in the regulation of virus infection. Genes Dev. **16:**2465–2478.
12. **Dourmishev, L. A., A. L. Dourmishev, D. Palmeri, R. A. Schwartz, and D. M. Lukac.** 2003. Molecular genetics of Kaposi's sarcoma-associated herpesvirus (human herpesvirus-8) epidemiology and pathogenesis. Microbiol. Mol. Biol. Rev. **67:**175–212.
13. **Flanagan, A. M., and A. Letai.** 2008. BH3 domains define selective inhibitory interactions with BHRF-1 and KSHV BCL-2. Cell Death Differ. **15:**580–588.
14. **Granato, D. C., G. M. Machado-Santelli, and C. C. Oliveira.** 2008. Nop53p interacts with 5.8S rRNA co-transcriptionally, and regulates processing of pre-rRNA by the exosome. FEBS J. **275:**4164–4178.
15. **Gross, A., J. M. McDonnell, and S. J. Korsmeyer.** 1999. BCL-2 family members and the mitochondria in apoptosis. Genes Dev. **13:**1899–1911.
16. **Guo, J. Y., A. Yamada, T. Kajino, J. Q. Wu, W. Tang, C. D. Freel, J. Feng, B. N. Chau, M. Z. Wang, S. S. Margolis, H. Y. Yoo, X. F. Wang, W. G. Dunphy, P. M. Irusta, J. M. Hardwick, and S. Kornbluth.** 2008. Aven-dependent activation of ATM following DNA damage. Curr. Biol. **18:**933–942.
17. **Hsu, Y. T., and R. J. Youle.** 1997. Nonionic detergents induce dimerization among members of the Bcl-2 family. J. Biol. Chem. **272:**13829–13834.
18. **Huang, Q., A. M. Petros, H. W. Virgin, S. W. Fesik, and E. T. Olejniczak.** 2002. Solution structure of a Bcl-2 homolog from Kaposi sarcoma virus. Proc. Natl. Acad. Sci. U. S. A. **99:**3428–3433.
19. **Jamil, S., R. Sobouti, P. Hojabrpour, M. Raj, J. Kast, and V. Duronio.** 2005. A proteolytic fragment of Mcl-1 exhibits nuclear localization and regulates cell growth by interaction with Cdk1. Biochem. J. **387:**659–667.
20. **Kim, Y. J., Y. E. Cho, Y. W. Kim, J. Y. Kim, S. Lee, and J. H. Park.** 2008. Suppression of putative tumour suppressor gene GLTSCR2 expression in human glioblastomas. J. Pathol. **216:**218–224.
21. **Liang, C., P. Feng, B. Ku, I. Dotan, D. Canaani, B. H. Oh, and J. U. Jung.** 2006. Autophagic and tumour suppressor activity of a novel Beclin1-binding protein UVRAG. Nat. Cell Biol. **8:**688–699.
22. **Loh, J., Q. Huang, A. M. Petros, D. Nettesheim, L. F. van Dyk, L. Labrada, S. H. Speck, B. Levine, E. T. Olejniczak, and H. W. Virgin.** 2005. A surface groove essential for viral Bcl-2 function during chronic infection in vivo. PLoS. Pathog. **1:**e10.
23. **Masa, S. R., R. Lando, and R. Sarid.** 2008. Transcriptional regulation of the open reading frame 35 encoded by Kaposi's sarcoma-associated herpesvirus. Virology **371:**14–31.
24. **Morency, E., Y. Coute, J. Thomas, P. Texier, and P. Lomonte.** 2005. The protein ICP0 of herpes simplex virus type 1 is targeted to nucleoli of infected cells. Arch. Virol. **150:**2387–2395.
25. **Ojala, P. M., K. Yamamoto, E. Castanos-Velez, P. Biberfeld, S. J. Korsmeyer, and T. P. Makela.** 2000. The apoptotic v-cyclin-CDK6 complex phosphorylates and inactivates Bcl-2. Nat. Cell Biol. **2:**819–825.
26. **Okahara, F., H. Ikawa, Y. Kanaho, and T. Maehama.** 2004. Regulation of PTEN phosphorylation and stability by a tumor suppressor candidate protein. J. Biol. Chem. **279:**45300–45303.
27. **Okahara, F., K. Itoh, M. Ebihara, M. Kobayashi, H. Maruyama, Y. Kanaho, and T. Maehama.** 2005. Production of research-grade antibody by in vivo electroporation of DNA-encoding target protein. Anal. Biochem. **336:**138–140.
28. **Okahara, F., K. Itoh, A. Nakagawara, M. Murakami, Y. Kanaho, and T. Maehama.** 2006. Critical role of PICT-1, a tumor suppressor candidate, in phosphatidylinositol 3,4,5-trisphosphate signals and tumorigenic transformation. Mol. Biol. Cell **17:**4888–4895.
29. **Pattingre, S., A. Tassa, X. Qu, R. Garuti, X. H. Liang, N. Mizushima, M. Packer, M. D. Schneider, and B. Levine.** 2005. Bcl-2 antiapoptotic proteins inhibit Beclin 1-dependent autophagy. Cell **122:**927–939.
30. **Paulose-Murphy, M., N. K. Ha, C. Xiang, Y. Chen, L. Gillim, R. Yarchoan, P. Meltzer, M. Bittner, J. Trent, and S. Zeichner.** 2001. Transcription program of human herpesvirus 8 (Kaposi's sarcoma-associated herpesvirus). J. Virol. **75:**4843–4853.
31. **Sarid, R., T. Sato, R. A. Bohenzky, J. J. Russo, and Y. Chang.** 1997. Kaposi's sarcoma-associated herpesvirus encodes a functional bcl-2 homologue. Nat. Med. **3:**293–298.
32. **Scherl, A., Y. Coute, C. Deon, A. Calle, K. Kindbeiter, J. C. Sanchez, A. Greco, D. Hochstrasser, and J. J. Diaz.** 2002. Functional proteomic analysis of human nucleolus. Mol. Biol. Cell **13:**4100–4109.
33. **Schmidt-Kastner, R., C. Aguirre-Chen, T. Kietzmann, I. Saul, R. Busto, and M. D. Ginsberg.** 2004. Nuclear localization of the hypoxia-regulated pro-apoptotic protein BNIP3 after global brain ischemia in the rat hippocampus. Brain Res. **1001:**133–142.
34. **Schmitt, E., M. Beauchemin, and R. Bertrand.** 2007. Nuclear colocalization and interaction between bcl-xL and cdk1(cdc2) during G_2/M cell-cycle checkpoint. Oncogene **26:**5851–5865.
35. **Smith, J. S., I. Tachibana, U. Pohl, H. K. Lee, U. Thanarajasingam, B. P. Portier, K. Ueki, S. Ramaswamy, S. J. Billings, H. W. Mohrenweiser, D. N. Louis, and R. B. Jenkins.** 2000. A transcript map of the chromosome 19q-arm glioma tumor suppressor region. Genomics **64:**44–50.
36. **Sulis, M. L., and R. Parsons.** 2003. PTEN: from pathology to biology. Trends Cell Biol. **13:**478–483.
37. **Walensky, L. D.** 2006. BCL-2 in the crosshairs: tipping the balance of life and death. Cell Death Differ. **13:**1339–1350.
38. **Wei, Y., S. Pattingre, S. Sinha, M. Bassik, and B. Levine.** 2008. JNK1-mediated phosphorylation of Bcl-2 regulates starvation-induced autophagy. Mol. Cell **30:**678–688.
39. **Widmer, I., M. Wernli, F. Bachmann, F. Gudat, G. Cathomas, and P. Erb.** 2002. Differential expression of viral Bcl-2 encoded by Kaposi's sarcoma-associated herpesvirus and human Bcl-2 in primary effusion lymphoma cells and Kaposi's sarcoma lesions. J. Virol. **76:**2551–2556.
40. **Yim, J. H., Y. J. Kim, J. H. Ko, Y. E. Cho, S. M. Kim, J. Y. Kim, S. Lee, and J. H. Park.** 2007. The putative tumor suppressor gene GLTSCR2 induces PTEN-modulated cell death. Cell Death Differ. **14:**1872–1879.